Condensing Effect of Palmitic Acid on DPPC in Mixed Langmuir Monolayers

Gang Ma and Heather C. Allen*

Department of Chemistry, The Ohio State University, 100 West 18th Avenue, Columbus, Ohio 43210

Received June 28, 2006. In Final Form: October 10, 2006

The interaction between deuterated dipalmitoylphosphatidylcholine (DPPC-*d62*) and palmitic acid (PA) in mixed Langmuir monolayers is studied using vibrational sum frequency generation (VSFG) spectroscopy. Palmitic acid is an additive in exogenous lung surfactant preparations such as Survanta and Surfaxin. The effect of PA on the chain conformation and orientation of DPPC in the liquid-expanded and condensed phases is explored. A condensing effect of PA on DPPC is observed with VSFG. At 12 mN/m, DPPC-*d62* alone is in the liquid-expanded phase. Adding PA increases the conformational ordering of DPPC chains and causes DPPC to transition from the expanded phase into the condensed phase. At 42 mN/m, DPPC-*d62* and PA form a mixed structure in the condensed phase. The presence of PA decreases the chain tilt angle of DPPC, increasing the orientational ordering of DPPC chains. At 42 mN/m, there is also evidence from the frequency red shift of the PO_2^- symmetric stretch that the carboxyl group of PA forms a hydrogen bond with the phosphate group of DPPC in the condensed phase. From this work the effect of PA on DPPC is 2-fold: (1) PA increases the chain ordering of DPPC and promotes the LE and TC phase separation and (2) due to the miscibility between DPPC and PA in the condensed phase, PA decreases the collapse pressure.

Introduction

Mixed Langmuir monolayers are monomolecular films containing more than one film-forming chemical component.[1] They are excellent model systems for understanding intermolecular interactions in a well-defined two-dimensional environment. Studies of mixed Langmuir monolayers are relevant to a variety of scientific and industrial areas such as membrane biophysics, lung function, pharmaceutical science, food technology, and detergent technology.[2,3] The study presented here explores the intermolecular interaction between dipalmitoylphosphatidylcholine (DPPC) and palmitic acid (PA) in mixed Langmuir monolayers. The primary motivation of this work is to better understand lung surfactant function. However, knowledge gained can also provide insight for understanding fundamental issues with respect to mixed monolayer systems such as molecular packing and mechanisms of interaction. Vibrational sum frequency generation (VSFG) spectroscopy is employed in this study to provide molecular-level evidence for the existence of the intermolecular interactions between DPPC and PA, major components in replacement lung surfactant mixtures, and also to shed light on the mechanisms of these interactions.

Mammalian lung surfactant is a complex mixture of lipids and proteins secreted by alveolar type II epithelial cells into the alveolar space. It lines the air−alveolus interface by forming a surfactant monolayer. The presence of the lung surfactant monolayer allows the surface tension at the alveolar surface to reach near-zero values during exhalation, thereby easing the work of breathing and preventing collapse of the lung. Lung surfactant is critically important for proper lung mechanics.[4−7] Deficiency of lung surfactant in premature infants can result in the life threatening lung disorder neonatal respiratory distress syndrome (NRDS). In the United States, 50 000−60 000 infants are at risk for NRDS each year.[7] Current clinical treatment for NRDS is through surfactant replacement therapy, namely, administration of exogenous surfactants. Since its first use in human neonates about two decades ago, surfactant replacement therapy has been shown to improve the clinical outcome of infants at risk for NRDS.[7]

Exogenous lung surfactants used in surfactant replacement therapy can be classified into two types, animal-derived surfactant preparations and synthetic surfactant preparations.[7,8] These exogenous surfactants are not exact copies of the natural human lung surfactant, but several key components have been considered as important ingredients: saturated DPPC, unsaturated and anionic phosphatidylglycerol (PG), PA, and proteins, SP−B and SP−C (or their peptide analogues).[7,9] A clinically successful replacement surfactant may or may not contain all of the key components in its formulas. For example, the simplest synthetic surfactant, ALEC, only contains DPPC and egg PG.[7] Surfaxin, a synthetic surfactant preparation, contains DPPC, palmitoyloleoylphosphatidylglycerol (POPG), PA, and KL_4 (an analogue to SP−B).[7,8,10] Understanding the roles of these key components in lung surfactant has been a major motivation in lung surfactant research since this can provide a basis for the rational design of exogenous surfactants. The study performed here focuses on the role of PA in exogenous lung surfactant.

Previous studies have demonstrated the beneficial role of PA in replacement surfactant preparations.[9,11,12] Tanaka et al.

* To whom correspondence should be addressed. E-mail: allen@chemistry.ohio-state.edu.

(1) Gaines, G. L. *Insoluble Monolayers at Liquid−Gas Interfaces*; Interscience Publishers: New York, 1966.
(2) Birdi, K. S. *Self-Assembly Monolayer Structures of Lipids and Macromolecules at Interfaces*; Kluwer Academic/Plenum Publishers: New York, 1999.
(3) Dynarowicz-Latka, P.; Kita, K. *Adv. Colloid Interface Sci.* **1999**, *79*, 1.
(4) Goerke, J.; Clements, J. A. In *Handbook of Physiology: The Respiratory System*; Mackelm, P. T., Mead, J., Eds.; American Physiology Society: Washington, DC, 1986; Vol. III, p 247.
(5) Creuwels, L. A. J. M.; Van Golde, L. M. G.; Haagsman, H. P. *Lung* **1997**, *175*, 1.
(6) Veldhuizen, R.; Nag, K.; Orgeig, S.; Possmayer, F. *Biochim. Biophys. Acta* **1998**, *1408*, 90.
(7) Notter, R. H. *Lung Surfactants: Basic Science and Clinical Applications*; Marcel Dekker: New York, 2000.
(8) Pfister, R. H.; Soll, R. F. *Biol. Neonate* **2005**, *87*, 338.
(9) Tanaka, Y.; Takei, T.; Aiba, T.; Masuda, K.; Kiuchi, A.; Fujiwara, T. *J. Lipid Res.* **1986**, *27*, 475.
(10) Cochrane, C. G.; Revak, S. D. *Science* **1991**, *254*, 566.
(11) Holm, B. A.; Venkitaraman, A. R.; Enhorning, G.; Notter, R. H. *Chem. Phys. Lipids* **1990**, *52*, 243.

10.1021/la061870i CCC: $37.00
Published on Web 11/21/2006

investigated 26 surfactant preparations with a variety of lipid and protein compositions.[9] They found that surfactant mixtures containing PA had improved surface activity and adsorption rates as compared with surfactant mixtures without PA. Cockshutt et al. investigated the role of PA in the surface activity of lung surfactant and found that PA can greatly enhance the surface activity of lung surfactant preparations.[12] In addition, they also found that the PA-containing surfactant was more resistant to inhibitors such as fibrinogen, albumin, α-globulin, and lyso-PC. Due to the beneficial role of PA, PA has been an important additive in several exogenous lung surfactants including Survanta, Surfaxin, and recombinant SP−C surfactant.[7] Survanta is derived from bovine lung and supplemented with DPPC, PA, and tripalmitin. It contains 84 wt % phospholipids and 8 wt % PA. PA, as one of only four components in Surfaxin, has a concentration of 15 wt % relative to the phospholipids. The mole fraction of PA in these replacement surfactants is significant due to the relatively small molecular weight (M_w) of PA as compared to that of DPPC (M_w of PA is 256 amu and of DPPC is 734 amu).

The work presented here explores the effect of PA on DPPC in mixed Langmuir monolayers at the air−water interface. Mixed Langmuir monolayers have been widely used in lung surfactant research to investigate intermolecular interactions among lung surfactant components.[7,13] Since DPPC is the predominant lipid in lung surfactant and all of the exogenous lung surfactants incorporate it, investigating the effect of PA on DPPC has clear relevance for clarifying the possible role of PA in exogenous lung surfactant. In particular, the major goal in this work is to provide a molecular-level understanding about how PA affects the conformation and orientation of the DPPC molecules in different phases within the mixed monolayers. VSFG, a surface-selective spectroscopic technique, is employed here to gain the above information. By using chain perdeuterated DPPC (DPPC-*d62*), VSFG can specifically probe the chain conformation and orientation of DPPC without interference from the PA chain. In addition, the effect of PA on the phosphate group of DPPC is also explored with VSFG by tuning the infrared pulses to the fingerprint region.

VSFG is well suited for probing the interfacial structures of Langmuir monolayers and Langmuir−Blodgett films.[14−24] A brief description about the VSFG approach is provided as follows. VSFG utilizes two pulsed laser beams with different frequencies to probe the surface. The surface second-order process generates a third frequency at the sum of the two probing beams' frequencies. Usually one probe beam is in the visible region and the other is in the infrared region. When the infrared frequency is resonant with a vibrational mode of the molecule adsorbed at the surface,

Scheme 1. Chain Perdeuterated DPPC Molecule (DPPC-*d62*) (top) and Non-deuterated PA Molecule (bottom)

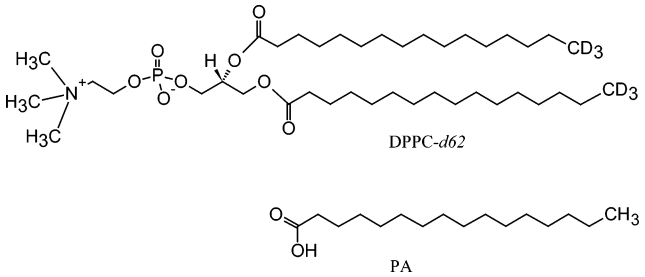

there is an SFG signal enhancement. VSFG has all the advantages of FTIR and Raman, yet it is also surface selective. The surface selectivity comes from the unique selection rule, requiring lack of inversion symmetry. The interface always satisfies this selection rule while the isotropic bulk does not. There are two types of VSFG technologies, scanning VSFG and broad bandwidth VSFG (BBSFG). In this study, BBSFG technology is used.

The VSFG intensity, I_{SFG}, as shown in eq 1

$$I_{SFG} \propto |\chi^{(2)}|^2 \propto |\chi_{NR}{}^{(2)} + \sum_v \chi_v{}^{(2)}|^2 \quad (1)$$

is proportional to the absolute square of the macroscopic second-order susceptibility, $\chi^{(2)}$, which consists of resonant terms ($\chi_v{}^{(2)}$) and a nonresonant term ($\chi_{NR}{}^{(2)}$). When the frequency of an incident infrared beam, ω_{IR}, is resonant with a vibrational mode, v, the resonant susceptibility term ($\chi_v{}^{(2)}$) dominates the nonlinear susceptibility ($\chi^{(2)}$) and an SFG intensity enhancement is observed.[16] The resonant macroscopic nonlinear susceptibility, $\chi_v{}^{(2)}$, is shown in eq 2

$$\chi_v{}^{(2)} \propto \frac{A_v}{\omega_{IR} - \omega_v + i\Gamma_v} \quad (2)$$

where A_v is the strength of the transition moment, ω_v is the frequency of the transition moment, and Γ_v describes the line width of the transition.[16] Since VSFG can be treated as an anti-Stokes Raman process on a vibrationally excited state, the strength, A_v, is nonzero when the Raman and the infrared transitions are spectroscopically allowed.[25] $\chi_v{}^{(2)}$ is related to the molecular hyperpolarizability, β_v, shown in eq 3, by the number density of the surface species, N, and an orientationally averaged Euler angle transformation, $\langle\mu_{IJK:lmn}\rangle$, between the laboratory coordinates (I, J, K) and the molecule-coordinates (l, m, n). The Euler angle transformation contains the molecular orientation information.[26]

$$\chi_v{}^{(2)} = N\sum_{lmn}\langle\mu_{IJK:lmn}\rangle\beta_v \quad (3)$$

Experimental Section

Materials. Acyl chain perdeuterated 1,2-dipalmitoyl-sn-glycero-3-phosphocholine (DPPC-*d62*) (Scheme 1) with >99% purity was obtained from Avanti Polar Lipids (Alabaster, AL). PA (Scheme 1) with a 99% purity was purchased from Sigma-Aldrich. Spectrophotometric-grade chloroform was purchased from Sigma-Aldrich. Deionized water (not purged of CO_2) was from a Barnstead Nanopure system with a resistivity of 18.2 MΩ·cm and a measured pH of 5.5.

Methods. *Langmuir Film Balance.* The surface pressure−area isotherm was obtained with a KSV minitrough (KSV, Finland). The rectangular trough (176.5 mm × 85 mm) is made of Teflon and

(12) Cockshutt, A. M.; Absolom, D. R.; Possmayer, F. *Biochim. Biophys. Acta* **1991**, *1085*, 248.
(13) Zasadzinski, J. A.; Ding, J.; Warriner, H. E.; Bringezu, F.; Waring, A. J. *Curr. Opin. Colloid Interface Sci.* **2001**, *6*, 506.
(14) Guyot-Sionnest, P.; Hunt, J. H.; Shen, Y. R. *Phys. Rev. Lett.* **1987**, *59*, 1597.
(15) Zhang, D.; Gutow, J.; Eisenthal, K. B. *J. Phys. Chem.* **1994**, *98*, 13729.
(16) Zhuang, X.; Miranda, P. B.; Kim, D.; Shen, Y. R. *Phys. Rev. B* **1999**, *59*, 12632.
(17) Gurau, M. C.; Castellana, E. T.; Albertorio, F.; Kataoka, S.; Lim, S.-M.; Yang, R. D.; Cremer, P. S. *J. Am. Chem. Soc.* **2003**, *125*, 11166.
(18) Watry, M. R.; Tarbuck, T. L.; Richmond, G. L. *J. Phys. Chem. B* **2003**, *107*, 512.
(19) Roke, S.; Schins, J.; Muller, M.; Bonn, M. *Phys. Rev. Lett.* **2003**, *90*, 128101/1.
(20) Liu, J.; Conboy, J. C. *J. Am. Chem. Soc.* **2004**, *126*, 8894.
(21) Bonn, M.; Roke, S.; Berg, O.; Juurlink, L. B. F.; Stamouli, A.; Mueller, M. *J. Phys. Chem. B* **2004**, *108*, 19083.
(22) Ye, S.; Noda, H.; Nishida, T.; Morita, S.; Osawa, M. *Langmuir* **2004**, *20*, 357.
(23) Holman, J.; Davies, P. B.; Nishida, T.; Ye, S.; Neivandt, D. J. *J. Phys. Chem. B* **2005**, *109*, 18723.
(24) Ma, G.; Allen, H. C. *Langmuir* **2006**, *22*, 5341.
(25) Moad, A. J.; Simpson, G. J. *J. Phys. Chem. B* **2004**, *108*, 3548.
(26) Hirose, C.; Akamatsu, N.; Domen, K. *Appl. Spectrosc.* **1992**, *46*, 1051.

Scheme 2. Experiment Set Up: VSFG with a Langmuir Trough

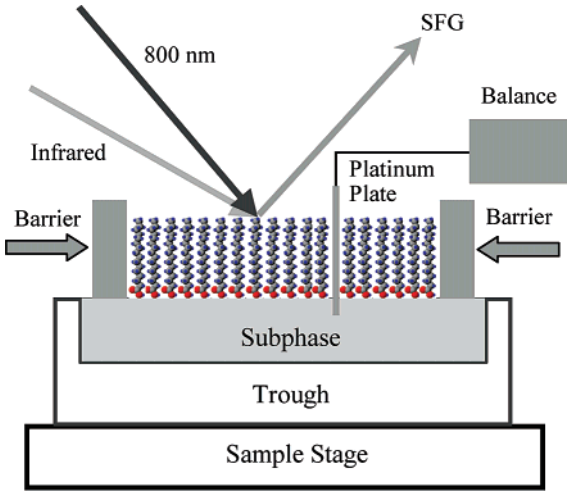

thermostated by circulating water in channels placed underneath the trough at a temperature of 24 ± 0.5 °C. Two barriers were employed to provide symmetric film compression. The barriers are made of Delrin, which prevents leakage of the monolayer beneath the barriers. The surface pressure and mean molecular area were continuously monitored during film compression by the Wilhelmy plate method. The plate was made of platinum and flamed by a Bunsen burner before use. The trough was filled with pure water as the subphase. The surface pressure−area isotherm was always measured on a fresh subphase. Before spreading lipids on the surface, the fresh subphase surface was swept by the barriers to make sure that there was no significant surface pressure increase observed upon compression. Stock solutions of DPPC-*d62* and PA were made in chloroform with a concentration of 1 mM. The DPPC-*d62*−PA mixture solutions were prepared by mixing desired amounts of the stock solutions of DPPC-*d62* and PA. Three different molar ratios of DPPC-*d62* to PA, 3:1, 1:1, and 1:3, were used in this study. These solutions were kept in a freezer at −20 °C when not being used. When preparing a Langmuir monolayer, a known amount of lipid solution was spread on the subphase surface in a dropwise manner with a Hamilton syringe and 10 min was allowed to elapse for complete solvent evaporation before starting the compression. A constant compression speed of 10 mm/min (corresponding to 5 mm/min barrier moving speed) was used during monolayer compression.

Vibrational Sum Frequency Generation (Broad Bandwidth Technology). The broad bandwidth VSFG system consists of two 1-kHz repetition rate regenerative amplifiers (Spectra-Physics Spitfire, femtosecond and picosecond versions), both of which are seeded by sub-50 fs 792 nm pulses (the wavelength is tuned for system optimization) from a Ti:sapphire oscillator (Spectra-Physics, Tsunami) and pumped by a 527 nm beam from an all solid-state Nd:YLF laser (Spectra-Physics, Evolution 30). The two regenerative amplifiers provide 85 fs pulses at 800 nm (22 nm bandwidth) and 2 ps pulses at 800 nm (17 cm^{-1} bandwidth). The femtosecond broad bandwidth pulses are then used to generate broad bandwidth infrared light via an optical parametric amplifier (Spectra-Physics, OPA-800CF). The spectral window of the broad IR pulse can be as large as 500 cm^{-1} depending on the tuned spectral region. Therefore, using a broad bandwidth VSFG system, a VSFG spectrum can be obtained without wavelength scanning. Tuning the nonlinear crystals (BBO and $AgGaS_2$) in the OPA cooperatively allows the IR output to cover different wavelength regions such as the C−D stretching region (2000−2300 cm^{-1}) and the PO_2^- symmetric stretching region (1000−1200 cm^{-1}). The output energy of each 800 nm ps pulse was 300 μJ, and the IR energies were 6 μJ in the C−D stretching region and 1 μJ in the PO_2^- symmetric stretching region.

The 800 nm ps beam and spectrally broad IR beam are the two probe laser beams of the VSFG system. As shown in Scheme 2, the Langmuir film balance is placed on the sample stage of the VSFG system. The two probe beams are overlapped at the monolayer surface spatially and temporally. The generated VSFG signal containing spectral information from the monolayer is detected using a monochromator-CCD detection system (Acton Research, SpectraPro SP-500 monochromator with a 1200 g/mm grating blazed at 750 nm; Roper Scientific, 1340 × 400 pixel array, LN400EB back-illuminated CCD). The VSFG spectrum is polarization dependent. In this study the polarization combination of ssp (s-SFG; s-800 nm; p-infrared) was used. The VSFG spectra were normalized against a nonresonant VSFG spectrum from a GaAs crystal (Lambda Precision Optics, Inc) to remove the spectral distortion caused by the energy profile of the infrared pulse. To calibrate the VSFG peak positions, a nonresonant VSFG spectrum from the GaAs crystal surface was obtained with a polystyrene film covering the OPA infrared output port. The resulting VSFG spectrum containing polystyrene infrared absorption bands was used for the calibration. The calibration accuracy is better than 1 cm^{-1}. The spectral resolution of the BBSFG system was characterized with an approach proposed by Ishibashi and Onishi and determined to be 8 cm^{-1}.[27]

When performing a VSFG study on the monolayer under different surface pressures, the spectra were taken either under the pause working mode of the film balance or the hold working mode of the film balance. In the pause mode, the monolayer was first compressed by the two barriers to reach a given surface pressure and then the barriers are halted and a VSFG spectrum was obtained. At low surface pressure (below the LE−TC phase transition of pure DPPC-*d62*, i.e., at 12 mN/m) the pause mode was used. At high surface pressure (above the LE−TC phase transition of pure DPPC-*d62*, i.e., at 42 mN/m) both modes were tested and identical spectra were obtained. In the pause mode a surface pressure drop is observed. In the hold mode the barriers move to compensate for the surface pressure drop and a constant surface pressure is retained. The surface pressure drop under the hold mode has been observed by other researchers when performing infrared reflection−absorption spectroscopy (IRRAS) studies on DPPC-containing monolayers.[28,29] Its effect on the VSFG spectra is negligible due to the relatively short data acquisition time (5 min) used in our study.

In this paper, we show representative VSFG spectra obtained at surface pressures of 12 and 42 mN/m from pure DPPC-*d62* monolayers and DPPC-62-PA mixed monolayers. The VSFG spectra of the monolayer were fit with Lorentzian line shapes according to eqs 1 and 2 using the commercial software IGOR after adding additional codes to describe the coherent nature of the SFG process.

Results and Discussion

Surface pressure−area isotherm measurements characterize the phase behavior of Langmuir monolayers.[1] Figure 1A shows the surface pressure−area isotherms of PA (left curve) and chain-deuterated DPPC-*d62* (right curve) at 24 °C on a pure water subphase. A number of distinct regions are shown in these isotherms. Each region is a separate phase.[1] Following the general assignments for the lipid phases in the literature,[30] the phases of DPPC-*d62* are assigned as G-LE, LE, LE−TC, TC, and collapse phases as denoted in Figure 1A. The phases of PA are assigned as G-TC, TC, untilted, and collapse phases as also denoted in Figure 1A. G is the gas phase; LE is the liquid-expanded phase; TC is the tilted-condensed phase (TC has been frequently called the liquid-condensed or LC phase); G-LE is the coexistence of G and LE; LE−TC is the coexistence of LE and TC. In the untilted phase the hydrocarbon chain of PA is perpendicular to the water surface. In the DPPC-*d62* isotherm the first-order LE−TC phase transition occurs at ∼15 mN/m for DPPC-*d62*. The film collapses at 63 mN/m. In the PA isotherm the asterisk at

(27) Ishibashi, T.-A.; Onishi, H. *Appl. Spectrosc.* **2002**, *56*, 1298.
(28) Cai, P.; Flach, C. R.; Mendelsohn, R. *Biochemistry* **2003**, *42*, 9446.
(29) Wang, L.; Cai, P.; Galla, H.-J.; He, H.; Flach, C. R.; Mendelsohn, R. *Eur. Biophys. J.* **2005**, *34*, 243.
(30) Kaganer, V. M.; Mohwald, H.; Dutta, P. *Rev. Mod. Phys.* **1999**, *71*, 779.

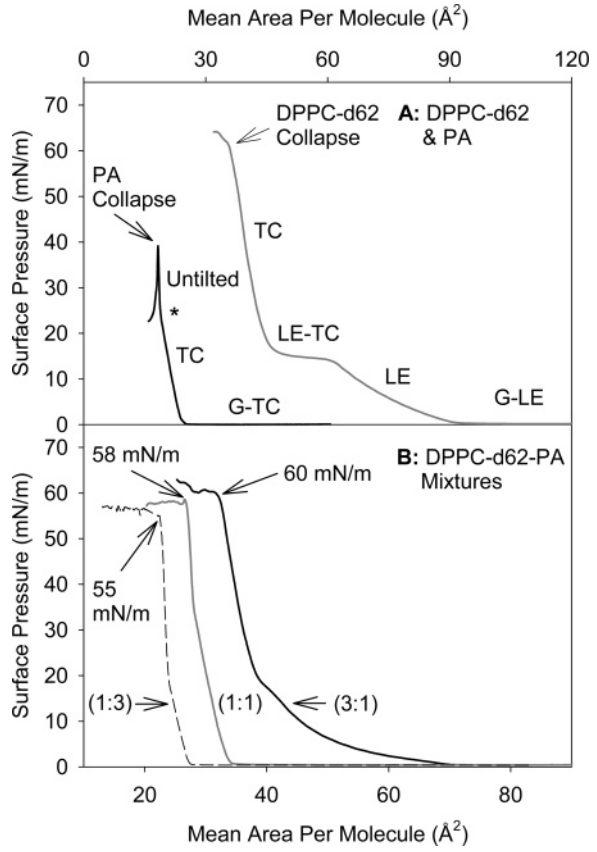

Figure 1. Surface pressure (mN/m)−area (Å²) isotherms at 24 °C on a pure water subphase: (A) neat DPPC-*d62* (gray curve) and neat PA (black curve), (B) mixtures of DPPC-*d62* and PA with three molar ratios (black curve, 3:1; gray curve, 1:1; dashed curve, 1:3). G, gas phase; LE, liquid-expanded phase; TC, tilted-condensed phase; Untilted, untilted-condensed phase; G-LE, coexistence of G and LE; G-TC, coexistence of G and TC; LE−TC, coexistence of LE and TC. All isotherms are the average of three measurements.

24 mN/m indicates the position of a kink, which is the second-order phase transition from the TC phase to the untilted condensed phase. The PA film collapses at a surface pressure of 40 mN/m.

Figure 1B shows the isotherms of DPPC-*d62*−PA mixed monolayers with different molar ratios of DPPC-*d62* to PA, namely, 3:1, 1:1, and 1:3. There are two obvious features in Figure 1B. The first feature is the variation of the collapse pressure with monolayer composition. The collapse pressures for the 3:1, 1:1, and 1:3 mixed monolayers are 60, 58, and 55 mN/m, respectively. According to the surface phase rule developed by Crisp,[1,3,31,32] the variation of the collapse pressure with composition in two-component mixed monolayers suggests miscibility. The second observation is that addition of PA diminishes the LE−TC transition plateau of DPPC-*d62*. For example, in the 1:1 and 1:3 curves, no plateau exits. If DPPC-*d62* and PA are ideally miscible (or completely immiscible), the isotherm of DPPC-*d62*−PA would be a simple summation of the two isotherms of neat DPPC-*d62* and PA according to their relative molar ratio. Therefore, the length of the plateau would only decrease with addition of PA, but it would not completely diminish as shown in Figure 1B. Its absence in Figure 1B indicates nonideal miscibility between DPPC-*d62* and PA in the mixed monolayers.

The surface pressure−area isotherms provide thermodynamic information about the interaction between DPPC-*d62* and PA.

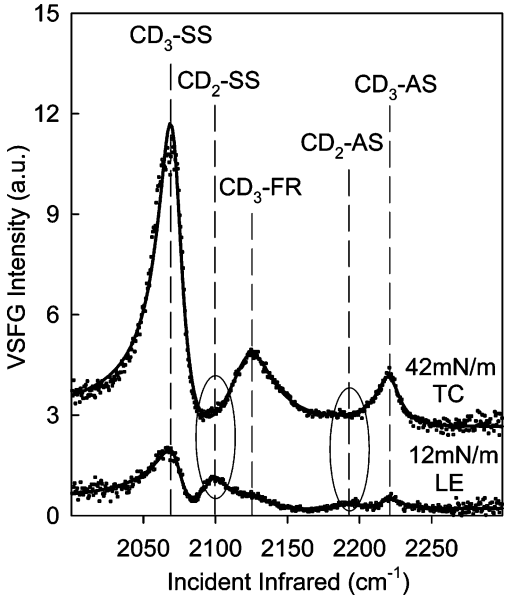

Figure 2. ssp VSFG spectra of the DPPC-*d62* monolayer in the C−D stretching region at different surface pressures. Solid curves are spectral fits. Dashed vertical lines reveal the spectral assignments: SS, symmetric stretch; FR, Fermi resonance; AS, asymmetric stretch. The spectral regions within the ellipses show the presence and absence of CD_2 stretches.

Table 1. Fitted Peak Frequencies and Assignments of the VSFG Spectra of DPPC-*d62* in LE Phase and TC Phase[a]

	CD_3-SS (cm^{-1})	CD_2-SS (cm^{-1})	CD_3-FR (cm^{-1})	CD_2-AS (cm^{-1})	CD_3-AS (cm^{-1})
12 mN/m (LE)	2073	2102	2121	2194	2221
42 mN/m (TC)	2071		2123		2221

[a] SS, symmetric stretch; AS, asymmetric stretch; FR, Fermi resonance.

However, to gain molecular-level insight into the specific intermolecular interaction, spectroscopic techniques are needed. In this study, vibrational sum frequency generation spectroscopy is employed to observe the intermolecular interactions between DPPC-*d62* and PA in the mixed monolayers.

As a starting point, the VSFG spectra of neat DPPC-*d62* were obtained at many surface pressures. Figure 2 shows the VSFG spectra of DPPC-*d62* with ssp polarization at two different surface pressures, 12 and 42 mM/m. The spectra were obtained in the C−D stretching region and therefore provide information about the conformation and orientation of the deuterated DPPC tails. The 12 mN/m VSFG spectrum is a representative spectrum of DPPC-*d62* in the LE phase; the 42 mN/m spectrum is a representative spectrum of DPPC-*d62* in the TC phase. Table 1 lists the peak positions from curve fits and the spectral assignments. At 12 mN/m, there are five peaks revealed in the spectrum located at 2073, 2102, 2121, 2194, and 2221 cm^{-1} as listed in Table 1. According to previous vibrational spectroscopic studies on deuterated DPPC,[33,34] these five peaks are assigned to CD_3-symmetric stretching (CD_3-SS), CD_2-symmetric stretching (CD_2-SS), CD_3 Fermi resonance (CD_3-FR), CD_2-asymmetric stretching (CD_2-AS), and CD_3-asymmetric stretching (CD_3-AS) modes, respectively. At 42 mN/m, only three peaks, CD_3-SS, CD_3-FR, and CD_3-AS, are observed in the VSFG spectrum.

The difference between the 12 mN/m (LE phase) VSFG spectrum and the 42 mN/m (TC phase) VSFG spectrum in Figure

(31) Crisp, D. J. In *Surface Chemistry Suppl. Research (London)*; Interscience Publishers Inc.: New York, 1949; p 17.
(32) Crisp, D. J. In *Surface Chemistry Suppl. Research (London)*; Interscience Publishers Inc.: New York, 1949; p 23.
(33) Sunder, S.; Cameron, D. G.; Casal, H. L.; Boulanger, Y.; Mantsch, H. H. *Chem. Phys. Lipids* **1981**, *28*, 137.
(34) Devlin, M. T.; Levin, I. W. *J. Raman Spectrosc.* **1990**, *21*, 441.

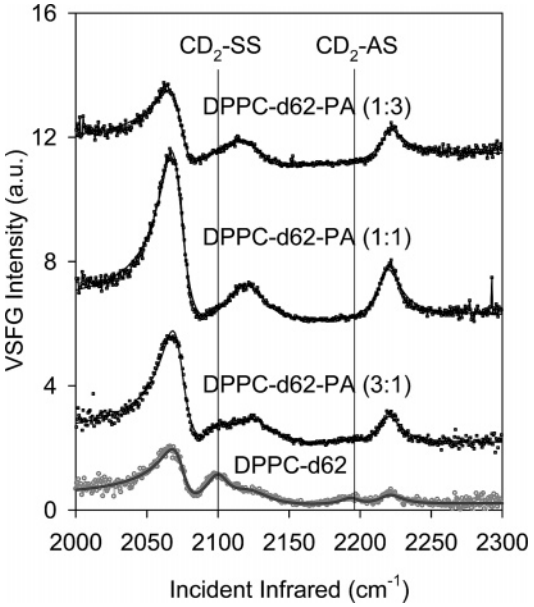

Figure 3. Surface pressure at 12 mN/m: ssp VSFG spectra of DPPC-*d62*−PA mixed monolayers in the C−D stretching region with three different molar ratios of DPPC-*d62* to PA. Solid curves are spectral fits. Vertical lines indicate peak positions of the CD_2-SS and CD_2-AS. Gray data points are the VSFG data of DPPC-*d62* at 12 mN/m from Figure 2 (reshown for comparison).

2 is due to the distinct structural difference of DPPC in the LE phase versus the TC phase. In the LE phase, DPPC molecules behave like a two-dimensional liquid. The fluidity of this phase causes the DPPC hydrocarbon tails to become disordered and adopt flexible gauche configurations. Recall the selection rule of lack of inversion symmetry mentioned in the Introduction; its application is well demonstrated here. At 12 mN/m, due to existence of the gauche configuration, the lack of inversion symmetry between each pair of gauche methylene groups allows both the CD_2-SS and CD_2-AS peaks to be SFG active, and therefore, the two peaks are clearly observed in the VSFG spectrum of 12 mN/m. In the TC phase, molecules are in a two-dimensional semicrystalline phase; the DPPC tails adopt an all-trans configuration. Since there are even numbers of methylene groups in the DPPC tail, no single methylene can be SFG active, and therefore, at 42 mN/m the CD_2-SS and the CD_2-AS peaks disappear, and only the CD_3-SS, CD_3-FR, and CD_3-AS peaks are observed in the VSFG spectrum.[24]

The basic strategy using VSFG to observe the DPPC−PA interaction is to investigate whether addition of PA into the DPPC monolayer will alter the VSFG spectrum of DPPC. If PA can alter the DPPC VSFG spectrum in some way, it suggests that there is an intermolecular interaction between DPPC and PA, or macroscopically, the miscibility between DPPC and PA is nonideal. The two VSFG spectra of pure DPPC monolayers in Figure 2 are the spectral references for the DPPC−PA interaction investigation, as shown in the following sections.

Figure 3 shows the VSFG spectra of DPPC-*d62* in the C−D stretching region in DPPC-*d62*−PA mixed monolayers at a surface pressure of 12 mN/m. For comparison, the 12 mN/m spectrum in Figure 2 is shown again in Figure 3 (the gray curve). The effect of PA on DPPC is well demonstrated in Figure 3. As indicated by the two vertical dashed lines, adding 0.25 mol fraction PA in DPPC (3:1 molar ratio between DPPC and PA) causes a substantial decrease of the CD_2-SS and CD_2-AS intensities as compared with the CD_3-SS and CD_3-AS intensities. Fitting results reveal that the relative intensity ratio of the CD_2-SS to the CD_3-SS ($I_{CD2-SS/CD3-SS}$) decrease significantly (from 0.5 to 0.03) in

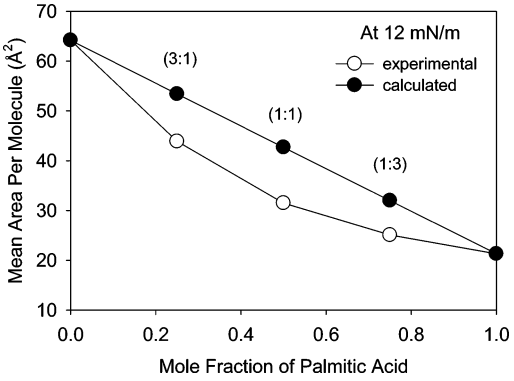

Figure 4. Mean area per molecule versus mole fraction of PA in DPPC-*d62*−PA mixtures. Open circles are the experimental values from isotherm measurements. Solid circles are calculated values by assuming an ideal miscibility between DPPC-*d62* and PA. All data points are the average of three measurements.

the DPPC-*d62*−PA (3:1) mixture; in addition, the relative intensity ratio of CD_2-AS to CD_3-AS ($I_{CD2-AS/CD3-AS}$) also decreases substantially (from 0.4 to 0.01). The relative intensity ratio drop between the methylene group and methyl group stretching bands in the VSFG spectrum qualitatively suggests an increase in chain ordering.[17,35,36] However, it is important to note that this spectral parameter can only be used as an empirical measure for the overall chain ordering. To further justify our interpretation, DPPC-*d62*−PA monolayers with increased PA concentrations were investigated. As shown in the VSFG spectra of the 1:1 and 1:3 mixtures of Figure 3, further increasing the PA concentration in the DPPC-*d62* monolayer results in additional spectral changes. In Figure 3, both the CD_2-SS and CD_2-AS nearly vanish, clearly demonstrating that the DPPC chains adopt a nearly all-trans configuration in these two mixed monolayers. Results here thus show that addition of PA induces the chain ordering of DPPC.

Figure 3 clearly shows that addition of PA induced an LE−condensed phase transition, transforming the expanded DPPC film to the condensed phase. This effect is generally referred to as a condensing effect, a phenomenon involving lipid−lipid interactions.[1] If assuming ideal miscibility or complete immiscibility between two lipids, the mean area per molecule in the two-component mixture at a given surface pressure can be calculated according to eq 4

$$A_{12} = X_1A_1 + X_2A_2 \tag{4}$$

In eq 4, A_{12} is the mean area per molecule in the two-component monolayer, X_1 and X_2 are the mole fractions of components 1 and 2, and A_1 and A_2 are the molecular areas of components 1 and 2 in their single-component monolayers at the same surface pressure. Negative deviation of the measured A (mean area per molecule) from A_{12} (calculated with eq 4) is called the condensing effect. When the condensing effect occurs at a given surface pressure, the lipid that is in the liquid-expanded phase by itself is the lipid to be condensed (for example, DPPC in this study). The other lipid (for example PA in this study) is the condensing agent. Figure 4 shows the mean molecular area versus monolayer composition diagram for the DPPC-*d62*−PA mixture. The straight line connects values of A_{12}, which are calculated based on the ideal miscibility between DPPC-*d62* and PA according to eq 4.

(35) Conboy, J. C.; Messmer, M. C.; Richmond, G. L. *J. Phys. Chem.* **1996**, *100*, 7617.
(36) Walker, R. A.; Conboy, J. C.; Richmond, G. L. *Langmuir* **1997**, *13*, 3070.

Scheme 3. Schematic Showing the Condensing Effect of PA on DPPC[a]

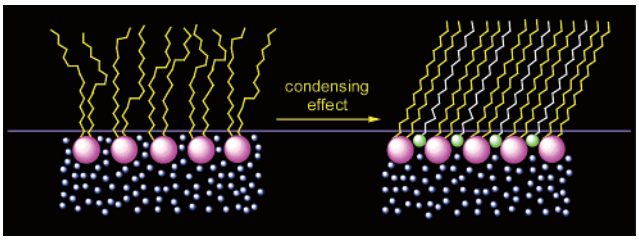

[a] Possible domain structures of the DPPC−PA system are not shown. The double-chain lipid molecule represents DPPC; the single-chain lipid molecule represents PA; the blue spheres represent water molecules.

The curved line connects the experimental values, *A*. The negative deviation from A_{12} caused by PA reveals a decreased mean molecular area with respect to the corresponding ideally mixed monolayers and demonstrates the condensing effect at a macroscopic level.

An interesting question is how does PA condense DPPC? The condensing effect between lipids has long been reported in the literature. Adam and Jessop used an intuitive way to explain the condensing effect.[1,37] They suggested that bulky or rigid molecules could mechanically impede the motions of more flexible molecules and hence reduce their tendency to expand. PA is in the condensed phase at 12 mN/m as indicated by the phase diagram in Figure 1A. The all-trans configuration of the chain makes PA a rigid molecule in the monolayer. We postulate that the rigid PA molecule can hinder rotational isomerization of the DPPC chains in the expanded phase and hence reduce or eliminate the number of gauche defects, forcing the neighboring DPPC molecules into a condensed phase. From a molecular-level viewpoint, the condensing effect is a PA-induced conformational ordering effect as depicted in Scheme 3. It is important to note that DPPC and PA are known to form domains at low PA concentrations (DPPC−PA of less than 1:1),[38] and therefore, the ordering effect in the 3:1 mixture is occurring in the DPPC−PA domains. When there is enough PA present in the DPPC−PA mixture, all of the DPPC molecules are forced into the condensed phase by PA. This is the case observed in Figure 3 for the 1:1 and 1:3 DPPC−PA mixtures. When there is not enough PA present in the DPPC−PA mixture as in the case of the 3:1 DPPC−PA mixture, there is a phase separation based on previous fluorescence microscopy studies by Lee et al.[38] The phase separation results in a coexistence of the LE phase and the condensed phase. A fraction of DPPC molecules exist with PA in the condensed phase domains, and others remain in the expanded phase. DPPC-*d62* molecules in the condensed domains do not produce SFG signal at the frequencies of the CD_2-SS and CD_2-AS. As shown in Figure 2, the LE−TC phase transition results in the disappearance of the methylene stretching peaks. Therefore, the PA-induced phase coexistence is consistent with the observed decrease in the methylene stretching intensities, which is clearly observed in the VSFG spectrum of the 3:1 DPPC−PA mixture in Figure 3.

At 42 mN/m, DPPC is in the TC phase and its chains are in an all-trans configuration but also tilted from the surface normal, consistent with the well-known head−tail size mismatch.[39−41] (Although one might expect the head−tail mismatch to induce gauche defects in the chains, the CD_2 peaks are not observed in these studies.) Adding the relatively small PA molecule may compensate for the pure DPPC head−tail mismatch to some extent. Figure 5 shows the VSFG spectra of DPPC-*d62* in mixed monolayers at 42 mN/m. Indeed, addition of PA causes changes in the DPPC-*d62* VSFG spectrum. To illustrate this point, the spectra shown in Figure 5 are normalized in a way that the peak heights of the CD_3-SS in all four spectra are the same (refer to the top dashed line). Clearly the relative ratios of the CD_3-AS to CD_3-SS increase with the increase of PA mole fraction in the mixed monolayers. The spectral variation of DPPC-*d62* caused by addition of PA suggests a nonideal miscibility between DPPC-*d62* and PA in the condensed phase. To quantify the effect of PA on DPPC-*d62*, orientation calculations on the CD_3 group were performed on the VSFG spectra shown in Figure 5.

The orientation angle θ of the terminal methyl group is a valuable piece of information that can be obtained from the VSFG spectrum. The angle θ can further be used to deduce the chain tilt angle α of DPPC with respect to the surface normal. VSFG orientation calculation methods have been well documented in the literature.[16,26] Briefly, the functional relationship between the VSFG second-order nonlinear susceptibility (χ) and the mean orientation angle (θ) forms the mathematical basis for the orientation calculation. The procedure requires solving simultaneous equations since θ is not the only unknown parameter. In the case of DPPC-*d62*, the orientation angle of the terminal CD_3 group, i.e., the angle between the C_3 axis of CD_3 and the surface normal, is calculated in the following way.

$$\chi_{yyz}(\mathrm{CD_3\text{-}SS}) = 1/2N\beta_{ccc}[\cos\theta(1+r) - \cos^3\theta(1-r)],\ r = \beta_{aac}/\beta_{ccc} \quad (5)$$

$$\chi_{yyz}(\mathrm{CD_3\text{-}AS}) = -N\beta_{caa}(\cos\theta - \cos^3\theta) \quad (6)$$

The second-order nonlinear susceptibility (χ) of the CD_3-SS and CD_3-AS are related to θ, surface molecular density (N), and the molecular hyperpolarizability (β) as described in eqs 5 and 6 where the ssp polarization combination is used in the VSFG measurement. The ratio between χ_{yyz} (CD_3−SS) and χ_{yyz} (CD_3-AS) has a direct relationship with θ (values of $r = 2.3$[15] and $\beta_{caa}/\beta_{aac} = 4.2$[42,43]). Therefore, θ can be easily obtained by knowing the ratio of χ_{yyz} (CD_3-SS) to χ_{yyz} (CD_3-AS). In practice, this ratio is obtained from the square root of the ratio of CD_3-SS to CD_3-AS peak intensities. To use the above method, it is assumed that the CD_3 group has C_{3v} symmetry, the surface is isotropic, and the orientation distribution is a δ function.

The calculated θ of the terminal methyl groups are listed in Table 2. In the all-trans methylene configuration the angle relationship between the chain axis and the C_3 axis of the terminal methyl is known to be about 41.5° (this is the average angle of the two chains deduced from recent literature[19]), and therefore, the chain tilt angle α with respect to the surface normal can be easily deduced from the relationship $\alpha = 41.5° - \theta$.[22,24]

As shown in Table 2, the calculated chain tilt angle of DPPC-*d62* in the TC phase is 25°, which is consistent with the value reported in a previous grazing incidence X-ray diffraction (GIXD) study by Lee et al.[38] This angle decreases with addition of PA. With the molar ratio of 1:3, the chain tilt angle of DPPC decreased

(37) Adam, N. K.; Jessop, G. *Proc. R. Soc. (London)* **1928**, *A120*, 473.
(38) Lee, K. Y. C.; Gopal, A.; von Nahmen, A.; Zasadzinski, J. A.; Majewski, J.; Smith, G. S.; Howes, P. B.; Kjaer, K. *J. Chem. Phys.* **2002**, *116*, 774.
(39) Gennis, R. B. *Biomembranes: Molecular Structure and Function*; Springer-Verlag: New York, 1989.
(40) Hauser, H.; Pascher, I.; Pearson, R. H.; Sundell, S. *Biochim. Biophys. Acta* **1981**, *650*, 21.
(41) Mohwald, H. *Annu. Rev. Phys. Chem.* **1990**, *41*, 441.
(42) Watanabe, N.; Yamamoto, H.; Wada, A.; Domen, K.; Hirose, C.; Ohtake, T.; Mino, N. *Spectrochim. Acta, A: Mol. Biomol. Spectrosc.* **1994**, *50A*, 1529.
(43) Wang, C.-Y.; Groenzin, H.; Shultz, M. J. *J. Phys. Chem. B* **2004**, *108*, 265.

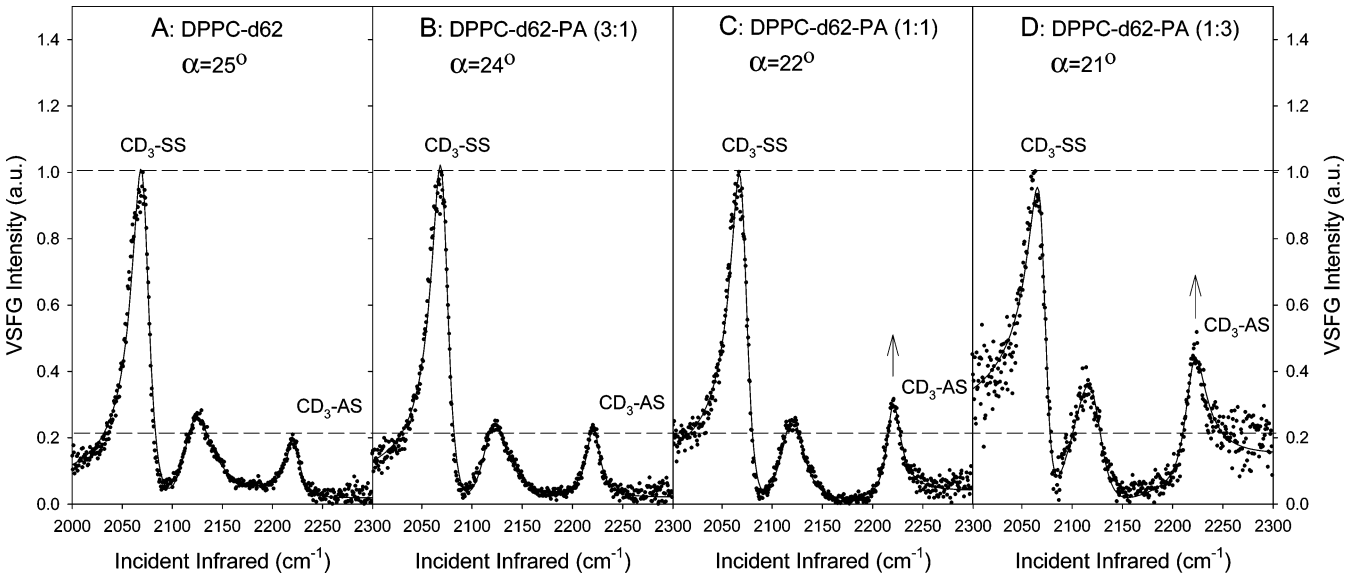

Figure 5. Surface pressure at 42 mN/m: ssp VSFG spectra of DPPC-*d62*−PA mixed monolayers in the C−D stretching region with three different molar ratios of DPPC-*d62* to PA. The VSFG spectrum of DPPC-*d62* at 42 mN/m from Figure 2 is shown for comparison. Solid curves are spectral fits. Dashed horizontal lines demonstrate the variation of the relative peak height ratio between CD_3-SS and CD_3-AS. α is the chain tilt angle with respect to the surface normal. (Spectra are scaled so that the CD_3-SS peaks have an intensity of unity. The seemingly significant baseline increase in Figure 5D is due to spectral rescaling.)

Table 2. At 42 mN/m: CD_3 Mean Orientation Angle (θ) and Chain Tilt Angle (α) Obtained from the VSFG Spectra of DPPC-*d62* and DPPC-*d62*−PA Mixtures with Different Molar Ratios[a]

DPPC-*d62* and DPPC-*d62*-PA Mixtures	θ (CD_3 orientation angle, deg)	α (chain tilt angle, deg)
DPPC-*d62*	16.4 ± 1	25
DPPC-*d62*-PA (3:1)	17.5 ± 1	24
DPPC-*d62*-PA (1:1)	19.5 ± 1	22
DPPC-*d62*-PA (1:3)	20.5 ± 1	21

[a] $\alpha = 41.5° - \theta$. The numbers in parentheses (3:1, 1:1, and 1:3) are molar ratios.

to 21°. The decreasing trend of the chain tilt angle induced by PA is also consistent with the GIXD study.[38]

As shown in eqs 4 and 5, the calculated tilt angle depends on r (β_{aac}/β_{ccc}) and β_{caa}/β_{aac}. There are inconsistencies for the two values reported in the literature. When choosing values from a recent study by Wang and co-workers ($r = 3.4$ and $\beta_{caa}/\beta_{aac} = 1$),[44] the calculated chain tilt angle of DPPC will correspondingly change from 25° to 9° (Supporting Information). These values are quite different. However, the variation of the tilt angle due to choosing different r and β_{caa}/β_{aac} values has no effect on the conclusion that addition of PA decreases the chain tilt angle of DPPC.

According to a previous phospholipid X-ray study,[40] the surface area occupied by the bulky headgroup of a PC is about 50 Å^2. On the other hand, the minimum cross-sectional area of the two hydrocarbon chains of a PC is about 38 Å^2. In a closely packed environment as in the TC phase, the chain must be tilted to some extent to compensate for the head−tail mismatch to form a stable monolayer at the air−water interface. Insertion of a relatively small molecule like PA into the DPPC condensed phase can compensate for the head−tail mismatch and reduce the chain tilt. Figure 5 serves as molecular-level evidence for formation of the mixed 2-dimensional semicrystalline structure of DPPC and PA and evidence for increased orientational ordering. The orientational ordering effect caused by PA can also be considered as a condensing effect since it decreases the mean area per DPPC hydrocarbon chain.

Long chain fatty acids have the capacity to form a hydrogen bond with the phosphate group of phosphatidylcholines.[45] PA at the air−water interface retains its COOH hydrogen. The pH of pure water is acidic enough to keep PA from being ionized due to its relatively high surface pK_a. The surface pK_a measured in a previous study by infrared spectroscopy was shown to be about 8.7 in phospholipid membranes.[46] Calculations based on Gouy−Chapman theory also showed that ionization of PA at the air−water interface is negligible.[47] Therefore, PA has available its COOH hydrogen to form a hydrogen bond with its neighbor lipids.

It is known that the headgroup of a lipid compressed into the condensed phase will be dehydrated.[1,15,24] For the dehydrated DPPC headgroup, if PA can form a hydrogen bond with this polar end, the headgroup spectral signature should experience a frequency shift to some extent. Figure 6 shows the VSFG spectra of the phosphate symmetric stretch of a DPPC monolayer and a DPPC−PA mixed monolayer at 42 mN/m. The peak assignment is based on previous infrared and Raman studies on phospholipids.[48−51] As demonstrated by the vertical line in Figure 6, adding PA causes the vibrational frequency of the DPPC phosphate symmetric stretch (PO_2^--SS) to be red shifted. Theoretical prediction has documented that hydrogen-bond formation to the phosphate group induces the loss of electron density of the PO_2^-, and consequently, there is an elongation of

(44) Wang, H.-F.; Gan, W.; Lu, R.; Rao, Y.; Wu, B.-H. *Int. Rev. Phys. Chem.* **2005**, *24*, 191.
(45) Seddon, J. M.; Cevc, G. In *Phospholipids Handbook*; Cevc, G., Ed.; Marcel Dekker: New York, 1993; p 403.
(46) Gomez-Fernandez, J. C.; Villalain, J. *Chem. Phys. Lipids* **1998**, *96*, 41.
(47) Lipp, M. M.; Lee, K. Y. C.; Waring, A.; Zasadzinski, J. A. *Biophys. J.* **1997**, *72*, 2783.
(48) Arrondo, J. L.; Goni, F. M.; Macarulla, J. M. *Biochim. Biophys. Acta* **1984**, *794*, 165.
(49) Harrand, M. *J. Chem. Phys.* **1984**, *81*, 1.
(50) Okamura, E.; Umemura, J.; Takenaka, T. *Biochim. Biophys. Acta* **1990**, *1025*, 94.
(51) Wong, P. T.; Capes, S. E.; Mantsch, H. H. *Biochim. Biophys. Acta* **1989**, *980*, 37.

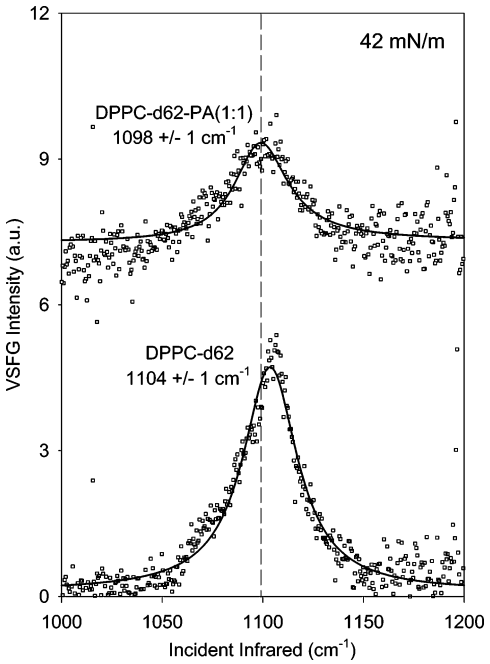

Figure 6. Surface pressure at 42 mN/m: ssp VSFG spectra in the PO_2^- symmetric stretching region of DPPC-*d62*−PA mixed monolayer (1:1 molar ratio) and DPPC-*d62*. Solid curves are spectral fits. Dashed vertical lines indicate the frequency red shift.

Scheme 4. Schematic Showing the Possible Hydrogen-Bond Formation between the Phosphate Group of DPPC-*d62* and the COOH Hydroxyl Group of PA

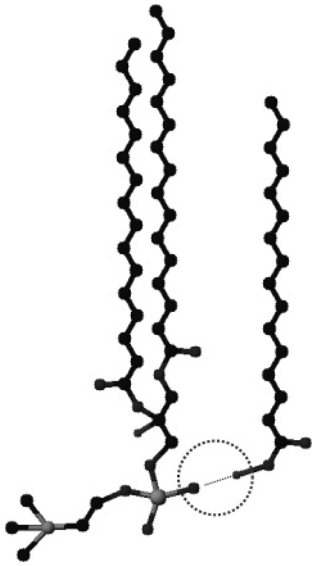

the $(O-P-O)^-$ bonds, causing a frequency red shift.[52] Therefore, consistent with theoretical prediction, our observed frequency red shift caused by PA (Figure 6) suggests possible hydrogen-bond formation between PA's COOH hydroxyl group and an oxygen of the PO_2^- group of DPPC, as illustrated in Scheme 4. Hydrogen-bond formation is supported by previous computer simulation studies revealing that the phosphate and carbonyl groups of DPPC form hydrogen bonds with the hydroxyl group of cholesterol.[53−55]

One of the fundamental questions in lung surfactant function is how the near-zero surface tension of the lung surfactant monolayer is achieved. The generally accepted theory, often referred to as the classical model, is the squeeze-out theory.[4,7,56] According to this theory, unsaturated lipids and proteins will be selectively removed or squeezed out from the lung surfactant monolayer during film compression, leaving a DPPC-rich monolayer capable of reaching near-zero surface tension. In recent years, modifications have been made to provide a more detailed picture about the squeeze-out theory by introducing the concept of a surface-associated reservoir or surface-associated multilayers.[29,57−63] These surface-associated three-dimensional structures are thought to be mediated by SP−B and SP−C proteins. Although being challenged by other theories, such as the supercompressed fluid model,[64−66] the classical model still seems to tie together many experimental observations.[29,57−63,67,68] In the study presented here, implication of the possible role of PA in exogenous lung surfactant is based on the classical model.

According to the surface phase rule,[1,31,32] a prerequisite of the squeeze-out process is a phase separation. In a lung surfactant monolayer, phase separation results in a DPPC-rich condensed (TC) phase and a DPPC-poor liquid-expanded (LE) phase.[13] The LE−TC balance significantly affects lung surfactant properties. Any lipid component, which can affect the phase separation, can play an important role in lung surfactant function according to the squeeze-out theory.

Implicated by this study, the role of PA in lung surfactant lies in its ability to increase the conformational ordering of DPPC at low surface pressures, as demonstrated in Figure 3. In the complex lung surfactant mixture, PA's ability to increase the conformational ordering of DPPC can counteract the fluidizing (or disordering) effect of unsaturated lipids and promote phase separation between DPPC and other unsaturated lipids with disordered chains, such as POPG. The implication drawn here is supported by a previous study performed by Zasadzinski and co-workers in which Brewster angle microscopy and fluorescence microscopy were used to investigate PA's effect on model monolayers containing DPPC, PA, and the unsaturated lipid, POPG. Results showed that PA promoted the LE−TC phase separation between DPPC and POPG.[69]

The implication discussed above focuses on the role of PA at low surface pressures. PA's role of promoting phase separation

(52) Mrazkova, E.; Hobza, P.; Bohl, M.; Gauger, D. R.; Pohle, W. *J. Phys. Chem. B* **2005**, *109*, 15126.
(53) Tu, K.; Klein, M. L.; Tobias, D. J. *Biophys. J.* **1998**, *75*, 2147.
(54) Smondyrev, A. M.; Berkowitz, M. L. *Biophys. J.* **1999**, *77*, 2075.
(55) Chiu, S. W.; Jakobsson, E.; Scott, H. L. *J. Chem. Phys.* **2001**, *114*, 5435.
(56) Keough, K. M. W. In *Pulmonary Surfactant: From Molecular Biology to Clinical Practice*; Robertson, B., Van Golde, L. M. G., Batenburg, J. J., Eds.; Elsevier: Amsterdam, 1992; p 109.
(57) von Nahmen, A.; Schenk, M.; Sieber, M.; Amrein, M. *Biophys. J.* **1997**, *72*, 463.
(58) Schurch, S.; Green, F. H.; Bachofen, H. *Biochim. Biophys. Acta* **1998**, *1408*, 180.
(59) Kruger, P.; Schalke, M.; Wang, Z.; Notter, R. H.; Dluhy, R. A.; Losche, M. *Biophys. J.* **1999**, *77*, 903.
(60) Ding, J.; Takamoto, D. Y.; von Nahmen, A.; Lipp, M. M.; Lee, K. Y. C.; Waring, A. J.; Zasadzinski, J. A. *Biophys. J.* **2001**, *80*, 2262.
(61) Takamoto, D. Y.; Lipp, M. M.; von Nahmen, A.; Lee, K. Y. C.; Waring, A. J.; Zasadzinski, J. A. *Biophys. J.* **2001**, *81*, 153.
(62) Kruger, P.; Baatz, J. E.; Dluhy, R. A.; Losche, M. *Biophys. Chem.* **2002**, *99*, 209.
(63) Alonso, C.; Alig, T.; Yoon, J.; Bringezu, F.; Warriner, H.; Zasadzinski, J. A. *Biophys. J.* **2004**, *87*, 4188.
(64) Crane, J. M.; Hall, S. B. *Biophys. J.* **2001**, *80*, 1863.
(65) Smith, E. C.; Crane, J. M.; Laderas, T. G.; Hall, S. B. *Biophys. J.* **2003**, *85*, 3048.
(66) Rugonyi, S.; Hall, S. B. In *Lung Surfactant Function and Disorder*; Nag, K., Ed.; Taylor & Francis Group: Boca Raton, FL, 2005; p 173.
(67) Pastrana-Rios, B.; Flach, C. R.; Brauner, J. W.; Mautone, A. J.; Mendelsohn, R. *Biochemistry* **1994**, *33*, 5121.
(68) Brockman, J. M.; Wang, Z.; Notter, R. H.; Dluhy, R. A. *Biophys. J.* **2003**, *84*, 326.
(69) Bringezu, F.; Ding, J.; Brezesinski, G.; Zasadzinski, J. A. *Langmuir* **2001**, *17*, 4641.
(70) Alonso, C.; Bringezu, F.; Brezesinski, G.; Waring, A. J.; Zasadzinski, J. A. *Langmuir* **2005**, *21*, 1028.

between DPPC and other unsaturated lipids is thought to be beneficial to lung surfactant function since the squeeze out of unsaturated lipids helps lung surfactant to reach the near-zero surface tension.

What is the role of PA after the occurrence of the squeeze-out process? Following the above discussion, after unsaturated lipids are squeezed out, the DPPC−PA-rich film will remain at the surface. Due to the miscibility between DPPC and PA in the condensed phase, as demonstrated by Figure 5, the negative effect of PA on lung surfactant is revealed. According to the surface phase rule,[1,3,31,32] the collapse pressure of the mixed monolayer of DPPC−PA will lie between the collapse pressures of DPPC and PA and vary with the monolayer composition. Since PA's collapse pressure is only 40 mN/m, the collapse pressure of the DPPC and PA mixed film will certainly drop below 70 mN/m. The collapse pressure drop has been demonstrated by the isotherm measurements in Figure 1B. The collapse pressure drop due to the miscibility between DPPC and PA has a clear negative (or harmful) effect on lung surfactant function because it prohibits the DPPC−PA-rich monolayer from attaining near-zero surface tension. This collapse pressure drop in model lung surfactant monolayers induced by PA has also been observed by Bringezu et al.[69] In addition, the collapse pressure drop in a calf lung surfactant monolayer induced by hexadecanol (an analogue to PA) has also been reported recently by Alonso et al.[70] To avoid the collapse pressure drop of PA-containing lung surfactant monolayers, PA's negative effect must be controlled in some way. One way to control this effect is to keep the concentration of PA low in the replacement surfactant preparations. In addition, previous studies demonstrated that a surfactant protein may function to control the negative effect of PA in some way. Zasadzinski and co-workers investigated the effect of the SP−B protein on the collapse pressure of PA and showed that SP−B caused the collapse pressure of the DPPC−PA−SP−B mixed monolayer to be comparable to that of a pure DPPC monolayer and higher than that of a DPPC−PA mixed monolayer.[71,72] Demonstrated by their results, SP−B can be the agent in lung surfactant preparations that will contain the harmful effect of PA on monolayer collapse pressure by specifically interacting with PA.

(71) Longo, M. L.; Bisagno, A. M.; Zasadzinski, J. A.; Bruni, R.; Waring, A. J. *Science* **1993**, *261*, 453.

(72) Lipp, M. M.; Lee, K. Y.; Zasadzinski, J. A.; Waring, A. J. *Science* **1996**, *273*, 1196.

In summary, on one hand, PA increases the chain ordering of DPPC and promotes the phase separation between DPPC and other unsaturated lipids. This is beneficial for lung surfactant function. On the other hand, due to the miscibility between DPPC and PA in the condensed phase, PA decreases the collapse pressure of the lung surfactant monolayer. To contain the harmful effects from PA and exploit the beneficial effects of PA, there must be a balance between PA and other components and an optimal concentration of PA in replacement surfactant preparations.

Conclusions

The intermolecular interaction between DPPC-*d62* and PA in mixed Langmuir monolayers at the air−water interface is studied utilizing a surface-selective spectroscopy, vibrational sum frequency generation. The effects of PA on DPPC-*d62* in the LE and TC phases are explored by investigating the mixed monolayer under two different surface pressures, 12 and 42 mN/m. A condensing effect of PA on DPPC is observed with VSFG with addition of PA. At 12 mN/m, DPPC-*d62* alone is in the LE phase. Results showed that adding PA increased the conformational ordering of the DPPC hydrocarbon chains and consequently decreased the mean area per molecule in the mixed monolayer. At 42 mN/m, DPPC-*d62* alone is in the TC phase. Adding PA decreased the chain tilt angle of DPPC; specifically, it increased the orientational ordering of the DPPC chains. There is also evidence from the frequency red shift of the PO_2^- symmetric stretch that PA forms a hydrogen bond with the phosphate group of DPPC in the condensed phase. Implicated from this work, PA's effect on DPPC is 2-fold in lung surfactant function. PA increases the chain ordering of DPPC and promotes phase separation, which is thought to be beneficial to lung surfactant function. However, due to the miscibility between DPPC and PA in the condensed phase, PA can decrease the collapse pressure of the lung surfactant monolayer. This harmful effect of PA must be controlled during lung surfactant action.

Acknowledgment. The authors acknowledge the Arnold and Mabel Beckman Foundation for funding this research through a Beckman Young Investigator Award.

Supporting Information Available: VSFG spectra with error bars for data points (Figures S1−S4) and orientation calculations using different sets of literature values of r (β_{aac}/β_{ccc}) and β_{caa}/β_{aac} (Table S1). This material is available free of charge via the Internet at http://pubs.acs.org.

LA061870I